Journal of Biomolecular NMR, **14:** 169–174, 1999.
KLUWER/ESCOM

A high-resolution HCANH experiment with enhanced sensitivity via multiple quantum line narrowing

Göran Larsson, Sybren S. Wijmenga* & Jürgen Schleucher*
Department of Medical Biochemistry and Biophysics, Umeå University, S 901 87 Umeå, Sweden

Received 20 January 1999; Accepted 18 March 1999

Key words: calmodulin, HCANH, multiple quantum line narrowing, NMR assignment, resolution, SEF2-1

Abstract

We report a 3D constant-time HCANH experiment (CTSL-HCANH) that uses the slower relaxation of multiple-quantum coherence to increase sensitivity and provides high C^{α} resolution. In this experiment the H^{α} of the (H^{α}, C^{α}) multiple quanta are selectively spin locked, so that H^{α} chemical shift evolution and ^{1}H-^{1}H J-dephasing become ineffective during the relatively long delay needed for C^{α} to N coherence transfer. As compared to an HCANH experiment that uses C^{α} single-quantum coherence, an average enhancement of 20% was observed on calmodulin in complex with the binding domain of the transcription factor SEF2-1. Compared to CBCANH the signal intensity is approximately twice as good. The favorable relaxation properties of multiple quanta, together with the outstanding C^{α} resolution, make the experiment a very good complement to CBCANH and CBCA(CO)NH for sequential assignment of larger proteins for which deuteration is not yet necessary.

Backbone sequential assignment of ^{13}C, ^{15}N double-labeled proteins is nowadays mainly based on triple resonance experiments (for a recent review see Sattler et al., 1999). They can be divided into two groups. The first consists essentially of HNCA and HN(CO)CA experiments that use real-time (RT) C^{α} evolution. The second group of experiments is based on CBCA(CO)NH (Grzesiek and Bax, 1992a) and CBCANH (Grzesiek and Bax, 1992b). The presence of C^{β} correlations in the latter experiments resolves ambiguities in the sequential assignment. In addition, they show improved C^{α} resolution because constant-time (CT) carbon evolution is used. Nevertheless, congestion in the C^{α} region still often hinders manual or automated sequential assignment. Sequential assignment can therefore benefit from a sensitive experiment with high C^{α} resolution. This is achieved here in a constant-time HCANH experiment (CTSL-HCANH) by using the improved relaxation properties of multiple-quantum coherences.

*To whom correspondence should be addressed. E-mail: sybren@indigo.chem.umu.se; jurgen@rabbit.chem.umu.se

The main source of relaxation for ^{13}C nuclei in proteins, is usually the large ^{1}H-^{13}C dipolar interaction (relaxation rate $R_{C,Hdip}$). This large dipolar interaction is active when the ^{13}C spins are in single-quantum states (SQ). Both of the aforementioned groups of sequential assignment experiments employ SQ carbon coherence, which adversely affects their sensitivity. In two-spin, zero- and double-quantum coherences (multiple quanta, MQ) the ^{1}H-^{13}C dipolar coupling is, to first order, not active in the slow tumbling limit ($\omega_{H,C}\tau_c \gg 1$) (Ernst et al., 1987; Griffey and Redfield, 1987; Grzesiek and Bax, 1995). In this limit MQ relaxation is governed by proton homonuclear dipolar relaxation (relaxation rate $R_{H,H}$) and the ratio $R_{C,Hdip}/R_{H,H}$ has a constant value which depends on the local proton density. In the usual proton environment in proteins $R_{C,Hdip}/R_{H,H} > 1$. For BPTI, this ratio is approximately 1.3 on average (Grzesiek and Bax 1995). Thus, by preparation of MQ coherences, rather than SQ coherences, the slower MQ ^{13}C relaxation can be used to increase the sensitivity of NMR experiments.

(^{1}H,^{13}C) MQ coherence can evolve the chemical shift of both nuclei. The chemical shift evolution of ei-

ther nucleus can be refocused by 180° pulses. (^{1}H,^{13}C) MQ can also evolve under ^{1}H-^{1}H and long-range ^{1}H-^{13}C couplings, which leads to multiplet splittings in experiments with RT chemical shift evolution. In experiments with CT carbon evolution (of duration $2T_C$), each ^{1}H-^{1}H coupling instead reduces the transfer amplitude by a factor $\cos(\pi 2T_C J_{HH})$. To avoid the sensitivity loss caused by dephasing of the (H^α,C^α) MQ coherence by ^{1}H-^{1}H couplings, the H^α protons of the MQ coherence can be selectively spin locked (Grzesiek and Bax, 1995). In practice, the spin lock has to be chosen strong enough to spin lock all H^α spins, but weak enough to decouple H^α from H^β and H^N. For proteins both conditions can be fulfilled with a CW spin-lock field strength of around 5 kHz.

A good candidate to use spin-lock MQ line narrowing is the HCANH experiment, which transfers magnetization in a straight-through fashion from H^α, via C^α and N to H^N (Kay et al., 1991; Boucher et al., 1992; Montelione et al., 1992; Clowes et al., 1993; Grzesiek and Bax, 1993). Figure 1A shows the constant-time HCANH experiment (CT-HCANH) described by Feng et al. (1996). This version uses SQ C^α chemical shift evolution. The carbon CT period, $2T_C$, is used to refocus the H^α-C^α coupling, defocus C^α-N couplings and for C^α chemical shift evolution. The transfer function for the $C^\alpha \rightarrow$ N coherence transfer of the inter-residual cross peak is:

$$\sin(2\pi^2 J_{C\alpha N} T_C)\cos(2\pi^1 J_{C\alpha N} T_C)$$

$$\cos(2\pi J_{C\alpha C\beta} T_C) X \qquad (1)$$

Here, X is an experiment-specific term, which for the pulse sequence of Figure 1A is given by $\exp(-2T_C/T_{2,SQ})$, where $T_{2,SQ} \approx 1/R_{C,Hdip}$. Because the refocusing of C^α-H^α coupling occurs during the first part of $2T_C$, the C^α magnetization spends most of the delay $2T_C$ as a SQ coherence, giving rise to the relaxation term $\exp(-2T_C/T_{2,SQ})$. As discussed by Feng et al. (1996), the C^α constant time, $2T_C$, can be chosen as 7 ms or 24 ms (assuming typical values for $^2J_{C\alpha_N}$, $^1J_{C\alpha_N}$ and $J_{C\alpha_C\beta}$ of 7, 11, 35 Hz, $T_{2,SQ} = 20$ ms), so that either the C^α-C^β coupling does not evolve or is refocused. The latter choice offers much higher C^α resolution and better C^α to N transfer, but the fast SQ relaxation during $2T_C$ reduces the signal intensity.

To improve the sensitivity, the SQ C^α evolution can be replaced by MQ C^α evolution. This was done in the multiple-quantum constant-time HCANH experiment proposed by Swapna et al. (1997), using non-selective proton 180° pulses to refocus proton chemical shift evolution. The transfer function of this experiment is given by Equation 1, with $X = \exp(-2T_C/T_{2,MQ}) \Pi_i \cos(2\pi T_C J_{H\alpha_H} i)$, where $H^i = H^{\beta 1}$, $H^{\beta 2}$, H^N, and $T_{2,MQ}$ is the relaxation time of the (H^α,C^α) multiple quanta ($T_{2,MQ} \approx 1/R_{H,H}$). This factor X shows that the implementation with 180° pulses improves sensitivity via the longer relaxation time $T_{2,MQ}$. However, the sensitivity is reduced by the factor $\Pi_i \cos(2\pi T_C J_{H\alpha_H} i)$, which results from ^{1}H-^{1}H J-dephasing. For $2T_C = 24$ ms, this term equals 1/3 (assuming $J_{H\alpha_H}\beta 1 = 15$ Hz, $J_{H\alpha_H}\beta 2 = 6$ Hz, $J_{H\alpha_H} N = 8$ Hz). Therefore, $2T_C = 7$ ms had to be chosen by Swapna et al. to limit the sensitivity loss due to H^α-H^i couplings. Although the shorter carbon constant-time period reduces transverse relaxation, the side effect is a poorer C^α to N magnetization transfer (Equation 1). In all, this leads to non-optimal overall sensitivity combined with low C^α resolution.

The pulse sequence we propose is shown in Figure 1B. In this sequence, the SQ C^α evolution time of Figure 1A has been replaced by MQ C^α evolution, with a proton CW spin lock centered in the H^α region. Thus, the experiment becomes a constant-time spin lock HCANH (CTSL-HCANH). In this experiment, the C^α spins are in a MQ state for most of $2T_C$, while the C^α-H^α coupling is refocused in the final part of $2T_C$ by a 90° proton pulse followed by the delay δ_b. The factor X (Equation 1) is now given by $\exp(-2T_C/T_{2,MQ})$. Because the H^α-selective spin lock decouples H^α-H^i couplings, the factor $\Pi_i \cos(2\pi T_C J_{H\alpha_H} i)$ is absent, and the longer constant-time delay, $2T_C = 24$ ms, can be chosen. Furthermore, compared to the alternative choice, $2T_C = 7$ ms, the signal loss due to C^α relaxation is largely compensated by increased C^α to N coherence transfer, so that good sensitivity is achieved in combination with very high C^α resolution.

The experiment is demonstrated on calmodulin (CaM) in complex with the calmodulin binding domain of the basic helix-loop-helix transcription factor SL3 Enhancer factor 2–1 (SEF2-1) (Larsson et al., 1999), which has a molecular weight of 38 kDa, although it behaves as a 20–25 kDa complex. In the following, we compare the CTSL-HCANH experiment with regard to sensitivity and resolution with the established CT-HCANH, HNCA and CBCANH experiments.

The average gain in sensitivity between CTSL-HCANH and CT-HCANH was found to be approximately 20% (see Figure 2). The enhancement factor varied from 0.8 to 1.8 for different (non-glycine)

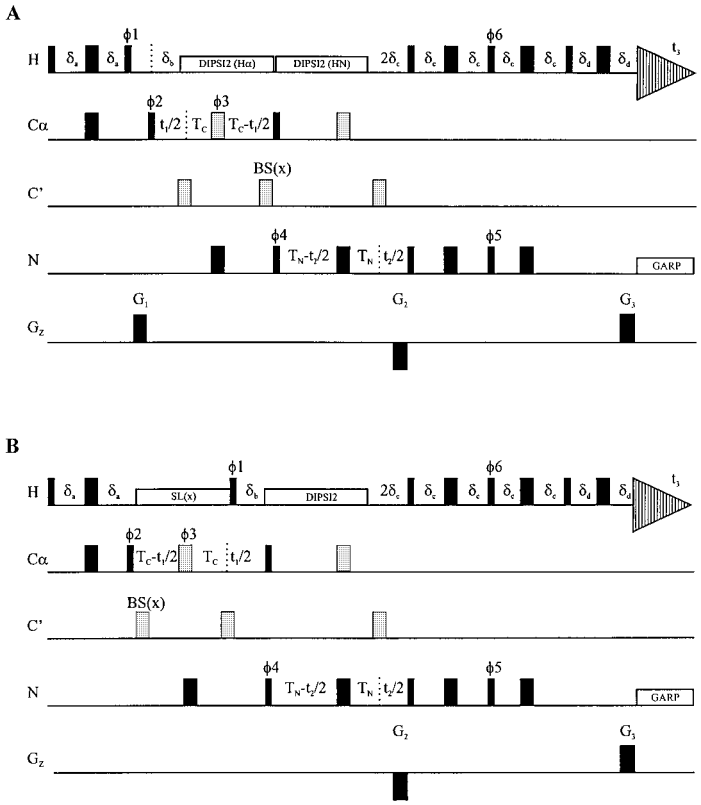

Figure 1. Pulse sequence of 3D (A) CT-HCANH and (B) CTSL-HCANH. Narrow and wide bars correspond to flip angles of 90° and 180°, respectively. Shaded bars correspond to selective G3 shaped pulses (Emsley and Bodenhausen, 1992) of 250 μs duration. The pulses marked BS compensate Bloch–Siegert phase shifts. The carbon carrier was placed at 54 ppm for C^{α} pulses, C′ pulses at 175 ppm were generated via phase modulation. The proton carrier was shifted from 4.24 ppm to 8.79 ppm after the carbon constant-time evolution period. The nitrogen carrier was placed in the middle of the amide region (118 ppm). Squared pulse field gradients of 500 μs duration were applied along the z-axis with strengths of $G_1 = 20$ G/cm, $G_2 = -30$ G/cm and $G_3 = 3$ G/cm (the G_2/G_3 ratio was optimized for maximum signal). The coherence transfer delays are: $\delta_a = 1.5$ ms, $\delta_b = 2.31$ ms, $\delta_c = 2.5$ ms, $\delta_d = 700$ μs, $T_C = 12.0$ ms and $T_N = 11.1$ ms. Unless indicated otherwise, all pulses are applied along the x-axis. The phase cycling scheme is: $\phi1 =$ y, y, −y, −y; $\phi2 =$ x, −x; $\phi3 = 8$(x), 8(y), 8(−x), 8(−y); $\phi4 = 4$(x), 4(−x); $\phi5 =$y; $\phi6 =$ y; Acq. = x, −x, −x, x, −x, x, x, −x, −x, x, x, −x, x, −x, −x, x. Quadrature detection in the indirect ^{13}C (t_1) dimension is obtained by States-TPPI (Marion et al., 1989) applied to phase $\phi2$ and in the ^{15}N (t_2) dimension by inverting the phase of $\phi5$ and G_3 simultaneously (Kay et al., 1992; Schleucher et al., 1993). Proton decoupling and proton spin lock are applied with $\gamma B_1/2\pi = 5$ kHz.

residues in the CaM:SEF2-1 complex and 90% of the cross peaks had increased signal-to-noise. The variation in enhancement is most likely due to variation in the proton-proton dipolar cross relaxation, because $T_{2,MQ} \approx 1/R_{H,H}$ is dependent on the local proton density. Considering the factors X in the transfer functions of the two experiments and the relevant parameter settings, the enhancement factors fall in the expected range and compare well with the enhancement factors observed by Grzesiek and Bax (1995) for spin-locked HMQC-type experiments on apo-calmodulin. Note that with increasing molecular weight the sensitivity enhancement will further improve, as follows from a comparison of the factors X in the transfer functions (Equation 1). The C^{α} resolution in the two experiments is the same, because $2T_C = t_{1,max} = 24$ ms in both.

A sensitivity comparison of the CTSL-HCANH with the HNCA experiment is difficult, because these experiments use constant-time and real-time C^{α} evolution periods, respectively. Taking this into account, we estimate from the intensities of the first FIDs of CTSL-HCANH and HNCA experiments that the CTSL-HCANH experiment is about half as sensitive as an HNCA experiment (Ikura et al., 1990). This is because the HNCA experiment is little affected by C^{α} relaxation, as the C^{α} evolution ($t_{1,max}$) is restricted to 7 ms due to the C^{α}-C^{β} coupling. The long constant-time C^{α} evolution that can be used in the CTSL-HCANH yields vastly improved resolution, compared

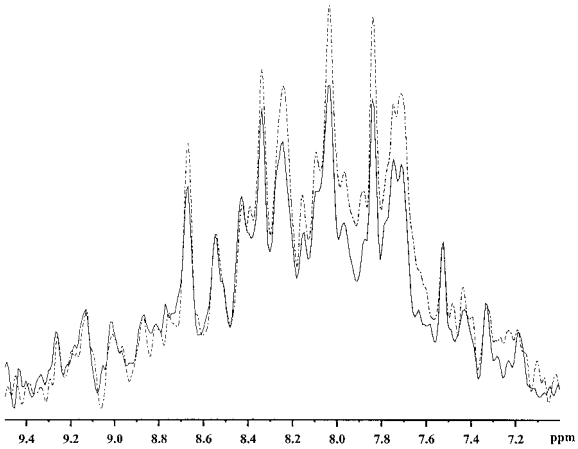

Figure 2. A comparison of the 1D traces of the first increment in the 2D C^{α}/H^{N} CT-HCANH (solid line) and the CTSL-HCANH (dashed line). The experiments were performed on a sample of uniformly $^{13}C,^{15}N$ labeled calmodulin in complex with the 21 amino acid binding domain of SEF2-1. All NMR experiments were conducted at 35 °C on a Bruker DRX-600 spectrometer equipped with a triple resonance ($^{1}H,^{13}C,^{15}N$) TXI probe with XYZ-gradient capabilities. The same spectral parameters and conditions were used for both experiments, and they were processed identically using the processing utilities within the XWINMR software on a Silicon Graphics workstation.

to the HNCA experiment. This gain in resolution between CTSL-HCANH and HNCA is demonstrated in Figure 3A and B, where expanded 2D C^{α}/H^{N} regions of CTSL-HCANH (3A) and HNCA (3B) experiments are compared. High C^{α} resolution can be crucial for assignment of proteins with poor C^{α} dispersion. Thus, the highly increased resolution, at an acceptable price in sensitivity, makes the CTSL-HCANH preferable to the HNCA experiment.

The signal intensity of the CTSL-HCANH is approximately twice as good as of the CBCANH. The improved sensitivity is illustrated in Figure 4. In the CBCANH (experiment time 4 days) shown in Figure 4A, both the C^{α} intra- and inter-residual peaks are missing from the N, H^{N} strip corresponding to I100 of CaM in the CaM:SEF2-1 complex, while they are clearly present in the CTSL-HCANH spectrum (experiment time 2.5 days) as shown in Figure 4B. The high resolution of the CTSL-HCANH experiment can resolve C^{α} resonances, which are not resolved in the CBCANH. This is demonstrated in Figure 4C and 4D for the sequential connectivity between S101 and A102. In the CBCANH spectrum (Figure 4C) the intraresidual and sequential C^{α} peaks for A102 overlap and peak picking would result in only one peak at a chemical shift position that fits neither A102 nor S101. The higher resolution in the CTSL-HCANH (Figure 4D) nicely resolves these C^{α} peaks to the degree that both the intra-residual and the sequential C^{α} shift can be determined with high accuracy.

In summary, for the CaM:SEF2 complex the CTSL-HCANH, CT-HCANH, HNCA, CBCANH, and CBCA(CO)NH experiments have average relative sensitivities of approximately 1, 0.8, 2, 0.5 and 1. For the same experiments, the C^{α} resolution attainable under practical circumstance is given by the ratios of $t_{1,max}$: 24, 24, 7 (RT), 7 and 7.

The usefulness of experiments for sequential assignment depends on both sensitivity and C^{α} resolution. With increasing molecular weight CBCANH is the experiment that will fail first, while the alternative, more sensitive HNCACB experiment (Wittekind and Mueller, 1993), is still expected to work. Therefore, in a sequential assignment strategy for larger proteins, the combination CBCA(CO)NH and HNCACB (instead of CBCANH) is preferable. The two experiments give the inter- and intra-residue C^{α} and C^{β} connections, albeit with low resolution, slightly better or comparable to that of the HNCA (Figure 3B). Overlap in the C^{α} region due to the low resolution still often hinders unambiguous sequential assignment for larger proteins. This overlap can be overcome if the low-resolution C^{α} shifts are replaced by high-resolution C^{α} shifts from a CTSL-HCANH. Furthermore, the favorable relaxation properties of MQ coherences make the CTSL-HCANH a useful experiment up to molecular weights where deuteration becomes necessary. Therefore, we suggest that the optimal combination of experiments would be CTSL-HCANH together with HNCACB and CBCA(CO)NH.

Cross peaks resulting from magnetization from glycines were found to have a decreased sensitivity in the CTSL-HCANH, compared with the CT-HCANH experiment. As discussed, (H^{α},C^{α}) MQ coherences relax essentially via proton-proton dipolar interaction. Consequently, the strong dipolar interactions between geminal protons considerably increase this relaxation rate. To remove this interaction and obtain MQ enhancement for glycines, the glycine $C^{\alpha}H_2$ spin moieties need to be in triple- and single-quantum states (Marino et al., 1997). This condition is not fulfilled in the CTSL-HCANH experiment. Hence, the intensities of glycine cross peaks are reduced, although all glycine C^{α} correlations are still observed for the CaM:SEF2-1 complex. In fact, all intra- and inter-residue correlations were observed. For larger proteins, missing glycine C^{α} correlations disrupt the

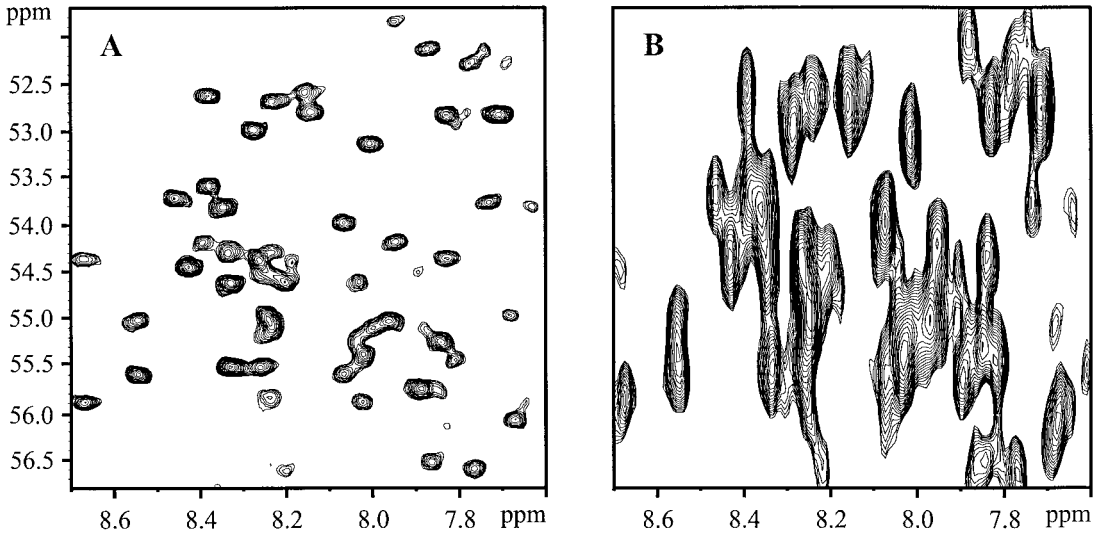

Figure 3. A comparison between a small C^{α}/H^{N} region of the 600 MHz spectra of the CTSL-HCANH (A) and the corresponding HNCA (B) experiment. The data set for (A) was acquired with 128 scans per FID and consists of 1024 × 170 real points. The ^{13}C dimension was linear predicted to 400 points and zero filled to 512 points prior to Fourier transformation. Both the ^{1}H and ^{13}C dimension were apodized with a phase-shifted squared sine bell. The spectrum for (B) was acquired with 32 scans per FID and consists of 1024 × 72 real points. The ^{13}C dimension was linear predicted to 128 points and zero filled to 256 points prior to Fourier transformation. Both the ^{1}H and ^{13}C dimension were apodized with a phase-shifted squared sine bell. Contour levels for both spectra are spaced by a factor of 1.2.

sequential walk. This hampers sequential assignment only if the peptide sequence between two glycines is not unique.

The CTSL-(H)CANH, i.e., the proposed experiment with C^{α} evolution, can be modified into a CTSL-H(CA)NH experiment with a CT H^{α} evolution of 12 ms duration, simply by replacing $\delta_a - 180°$ (H,C)-δ_a by $2\delta_a$ and the first part of the first delay T_C by $2\delta_a + t_{1/2} - 180°$(H)-$4\delta_a - t_{1/2}$, thereby delaying the onset of the H^{α} spin lock by $6\delta_a$.

The CTSL-HCANH experiment can also be modified into a 4D experiment with constant-time evolution for both H^{α} and C^{α}, so that MQ line narrowing can be used to improve sensitivity. This experiment would then form the MQ-enhanced version of the HCANNH proposed by Boucher et al. (1992), which is the 4D extension of the CT-HCANH experiment.

Boucher et al. (1992) compared SQ (C^{α},H^{α} HSQC) and MQ (C^{α},H^{α} HMQC) versions of RT 4D HNCAHA with SQ CT 4D HCANNH experiments and concluded that the SQ RT 4D HNCAHA should be preferred on the basis of C^{α} relaxation. As discussed above, the sensitivity of the CTSL-HCANH is approximately 50% of the RT HNCA. HNCAHA is less sensitive than HNCA, because of the additional C^{α},H^{α} transfer delays, while no additional delays are needed to introduce H^{α} evolution into CTSL-HCANH. Therefore, a high-resolution 4D CTSL-HCANH experiment is expected to be only slightly less sensitive than the low-resolution RT 4D HNCAHA.

However, the 4D CTSL-HCANH is inherently $\sqrt{2}$ less sensitive than the 3D versions. Moreover, the 4D version would sacrifice the good C^{α} or H^{α} resolution that can be obtained in the corresponding 3D experiments, because too few increments can be recorded in the 4D experiment in an affordable experiment time. Therefore, it is preferable to run two 3D CTSL-HCANH experiments, one with H^{α}- and one with C^{α}-CT evolution. The two 3D CTSL-HCANH experiments would give similar information as the 4D HCANNH experiment in the same amount of spectrometer time, but with much higher C^{α} and H^{α} resolution.

In conclusion, we have demonstrated an HCANH experiment using a constant-time C^{α} evolution of (H^{α},C^{α}) multiple quanta with a proton CW spin lock centered in the H^{α} region. The MQ implementation, as compared to the SQ implementation, shows an increase in sensitivity by a factor of 1.2 for non-glycine residues in the CaM:SEF2-1 complex. The use of the 24 ms long MQ CT C^{α} evolution combines two advantages, namely: (i) high enough sensitivity to assign proteins up to the molecular weight limit where deuteration is needed, and (ii) high C^{α} resolu-

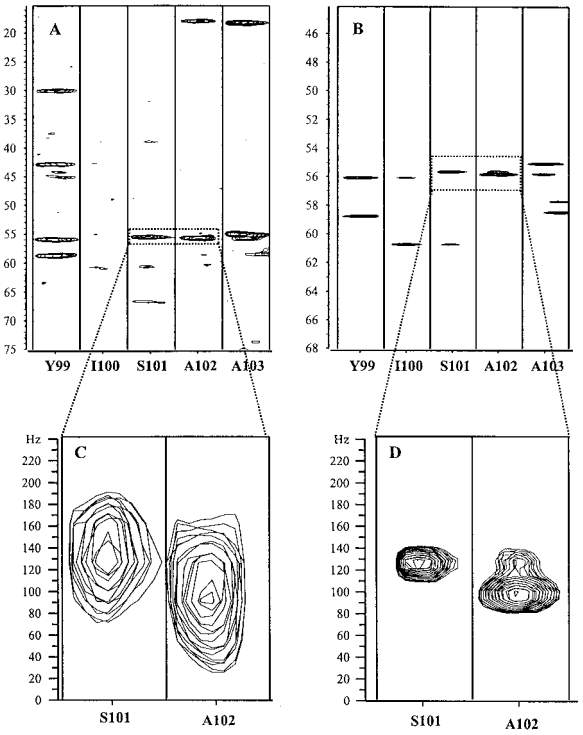

Figure 4. Strip plots from CBCANH (A) and CTSL-HCANH (B) experiments corresponding to calmodulin amino acids Y99 to A103 in the CaM:SEF2-1 complex. The CBCANH (A) was recorded with 800 (^{1}H) × 56 (^{15}N) × 110 (^{13}C) real points with 48 scans per FID with a total recording time of 98 h. The ^{15}N and ^{13}C dimensions were linear predicted to 100 and 200 points, respectively. Prior to Fourier transformation the spectrum was zero filled to a final data size of 1024 × 128 × 256 points and all dimensions were apodized with a phase-shifted squared sine bell. The CTSL-HCANH (B) was recorded with 1024 (^{1}H) × 62 (^{15}N) × 170 (^{13}C) real points with 16 scans per FID with a total recording time of 56 h. The ^{15}N and ^{13}C dimensions were linear predicted to 128 and 350 points respectively. Prior to Fourier transformation the spectrum was zero filled to a final matrix consisting of 1024×128×512 points and all dimensions were apodized with a phase-shifted squared sine bell. Panels C and D show expanded regions of panels A and B. In panel C the resonances of the intra- and inter-residual C^{α} shifts are overlapping, which results in one peak at an average chemical shift. As demonstrated in D, the higher resolution of the CTSL-HCANH resolves the overlapping peaks so that both the intra-residual and sequential C^{α} peaks can be determined with high accuracy.

tion to resolve overlap in the congested C^{α} spectral region. As a consequence, the CTSL-HCANH experiment is a good complement to the CBCANH or HNCACB experiments in sequential assignment. The high C^{α} resolution and the sequential connectivities it provides also make the CTSL-HCANH suitable for automatic assignment procedures. Such a procedure is in progress in our laboratory.

Acknowledgements

This work was supported by grants from the Swedish National Research Council (S.W.), the Bioteknik Medel Umeå University (S.W.) and the Kempe Foundation (G.L.).

References

Boucher, W., Laue, E.D., Campbell-Burk, S. and Domaille, P.J. (1992) *J. Biomol. NMR*, **2**, 631–637.

Clowes, R.T., Boucher, W., Hardman, C.H., Domaille, P.J. and Laue, E.D. (1993) *J. Biomol. NMR*, **3**, 349–354.

Emsley, L. and Bodenhausen, G. (1992) *J. Magn. Reson.*, **97**, 135–148.

Ernst, R.R., Bodenhausen, G. and Wokaun, A. (1987) *Principles of NMR in One and Two Dimensions*, Clarendon Press, Oxford, U.K.

Feng, W., Rios, C.B. and Montelione, G.T. (1996) *J. Biomol. NMR*, **8**, 98–104.

Griffey, R. and Redfield, A.G. (1987) *Q. Rev. Biophys.*, **19**, 51–82.

Grzesiek, S. and Bax, A. (1992a) *J. Am. Chem. Soc.*, **114**, 6291–6293.

Grzesiek, S. and Bax, A. (1992b) *J. Magn. Reson.*, **99**, 201–207.

Grzesiek, S. and Bax, A. (1993) *J. Biomol. NMR*, **3**, 185–204.

Grzesiek, S. and Bax, A. (1995) *J. Biomol. NMR*, **6**, 335–339.

Ikura, M., Kay, L.E. and Bax, A. (1990) *Biochemistry*, **29**, 4659–4667.

Kay, L.E., Ikura, M. and Bax, A. (1991) *J. Magn. Reson.*, **91**, 84–92.

Kay, L.E., Keifer, P. and Saarinen, T. (1992) *J. Am. Chem. Soc.*, **114**, 10663–10665.

Larsson, G., Schleucher, J., Onions, J., Hermann, S., Grundström, T. and Wijmenga, S.S. (1999) manuscript in preparation.

Marino, J.P., Diener, J.L., Moore, P.B. and Griesinger, C. (1997) *J. Am. Chem. Soc.*, **119**, 7361–7366.

Marion, D., Ikura, M., Tschudin, R. and Bax, A. (1989) *J. Magn. Reson.*, **87**, 183–188.

Montelione, G.T., Lyons, B.A., Emerson, S.D. and Tashiro, M. (1992) *J. Am. Chem. Soc.*, **114**, 10974–10975.

Sattler, M., Schleucher, J. and Griesinger, C. (1999) *Prog. Magn. Reson.*, **34**, in press.

Schleucher, J., Sattler, M. and Griesinger, C. (1993) *Angew. Chem. Int. Ed. Engl.*, **32**, 1489–1491.

Swapna, G.V.T., Rios, C.B., Shang, Z. and Montelione, G.T. (1997) *J. Biomol. NMR*, **9**, 105–111.

Wittekind, M. and Mueller, L. (1993) *J. Magn. Reson.*, **B101**, 201–205.